Structure of the Active Site of Sulfite Oxidase. X-ray Absorption Spectroscopy of the Mo(IV), Mo(V), and Mo(VI) Oxidation States

Graham N. George,*,‡ Cary A. Kipke,§,∥ Roger C. Prince,‡ Roger A. Sunde,⊥ John H. Enemark,§ and Stephen P. Cramer#

Exxon Research and Engineering Company, Annandale, New Jersey 08801, Department of Chemistry and Department of Nutrition and Food Science, University of Arizona, Tucson, Arizona 85721, and National Synchrotron Light Source, Brookhaven National Laboratory, Upton, New York 11973

Received December 6, 1988; Revised Manuscript Received March 3, 1989

ABSTRACT: The active site of sulfite oxidase has been investigated by X-ray absorption spectroscopy at the molybdenum K-edge at 4 K. We have investigated all three accessible molybdenum oxidation states, Mo(IV), Mo(V), and Mo(VI), allowing comparison with the Mo(V) electron paramagnetic resonance data for the first time. Quantitative analysis of the extended X-ray absorption fine structure indicates that the Mo(VI) oxidation state possesses two terminal oxo (Mo=O) and approximately three thiolate-like (Mo—S–) ligands and is unaffected by changes in pH and chloride concentration. The Mo(IV) and Mo(V) oxidation states, however, each have a single oxo ligand plus one Mo—O– (or Mo—N<) bond, most probably Mo—OH, and two to three thiolate-like ligands. Both reduced forms appear to gain a single chloride ligand under conditions of low pH and high chloride concentration.

Sulfite oxidase (EC 8.1.2.1) is responsible for the physiologically vital oxidation of sulfite to sulfate (Kessler & Rajagopalan, 1972; Bray, 1980, 1988). Residing in the mitochondrial intermembrane space, the enzyme is dimeric with a monomer molecular weight of about 55 000. Each monomer contains a single molybdenum cofactor and a cytochrome b_5 type heme. The two-electron oxidation of sulfite to sulfate presumably occurs at the molybdenum, which is reduced from the (resting) Mo(VI) oxidation state to Mo(IV) in the process

$$\text{Enz–Mo(VI)} + SO_3^{2-} + H_2O \rightarrow \text{Enz–Mo(IV)} + SO_4^{2-} + 2H^+$$

The catalytic cycle is completed by reoxidation of the molybdenum, first to Mo(V) and then to Mo(VI), by intramolecular electron transfer to the cytochrome *b* site (Kipke et al., 1988), which is reoxidized by intermolecular electron transfer to the physiological electron acceptor ferricytochrome *c*. The oxidation–reduction midpoint potentials (E_m) of the Mo(IV)/Mo(V), Mo(V)/Mo(VI) and ferro/ferricytochrome *b* couples have been determined by both redox potentiometry (Cramer et al., 1980) and microcoulometry (Spence, Kipke, Enemark, and Sunde, unpublished data) over a wide pH range and at different chloride concentrations.

The paramagnetic Mo(V) oxidation state of the enzyme has been extensively studied by electron paramagnetic resonance (EPR) spectroscopy (Cramer et al., 1979b; Lamy et al., 1980; Gutteridge et al., 1980; Bray et al., 1982, 1983). Four major Mo(V) EPR signals have been described, known as high-pH, low-pH, phosphate, and sulfite signals (Lamy et al., 1980; Bray et al., 1982). These EPR studies showed that the molybdenum site is sensitive to pH and to the anions chloride, sulfite, and phosphate and possesses oxygen ligands that are exchangeable with solvent water.

Previous EXAFS spectroscopy on sulfite oxidase (Cramer et al., 1979a, 1981) established that the molybdenum is ligated by two oxo groups plus two to three sulfur ligands in the Mo(VI) oxidation state and by a single oxo plus two to three sulfur ligands in the Mo(IV) oxidation state. However, the published EXAFS experiments were performed before the influences of anions and pH on the molybdenum site were properly appreciated. Thus, with the benefit of hindsight and using the properties of the Mo(V) oxidation state as a guide (Bray et al., 1983), we now believe that at least some of the original samples probably represented a mixture of phosphate-inhibited, high-pH, and low-pH species. A reinvestigation of the EXAFS of sulfite oxidase is therefore warranted. We present herein an EXAFS investigation of the molybdenum site in Mo(VI), Mo(V), and Mo(IV) oxidation states under conditions expected to yield predominantly high-pH and low-pH forms. Of particular importance is the X-ray spectroscopy of the Mo(V) forms, which allows a comparison of the X-ray and EPR data on the same species for the first time.

Experimental Procedures

Sample Preparation. Sulfite oxidase was prepared from chicken liver by a modification of the method of Kessler and Rajagopalan (1972) (Kipke et al., 1989), and activity was routinely monitored by the method of Cohen and Fridovich (1971). Typical molybdenum analyses of the purified enzyme, determined by atomic absorption spectroscopy using a Perkin-Elmer Zeeman/5000 spectrometer, gave Mo:heme ratios of 1.00:0.97.

Samples at pH 6 were prepared in a mixed buffer containing 20 mM Tris, bis-Tris, and bis-Tris–propane with 0.3 M KCl, while samples at pH 9 were prepared free of chloride in the same buffer. The fully oxidized samples, containing the (resting) Mo(VI) oxidation state, used the enzyme as prepared. Reduced samples were prepared anaerobically: samples in the Mo(V) oxidation state were poised at potentials of +65 mV, pH 6, and −131 mV, pH 9 (vs SHE) in the presence of 40 μM 1,2-naphthoquinone-4-sulfonate, duroquinone, pyocyanin, indigo trisulfonate, 2-hydroxy-1,4-naphtho- and anthraquinones,

‡ Exxon Research and Engineering Co.
§ Department of Chemistry, University of Arizona.
∥ Present address: Department of Chemistry, University of California, Berkeley, CA 94720.
⊥ Department of Nutrition and Food Science, University of Arizona.
Brookhaven National Laboratory.

0006-2960/89/0428-5075$01.50/0

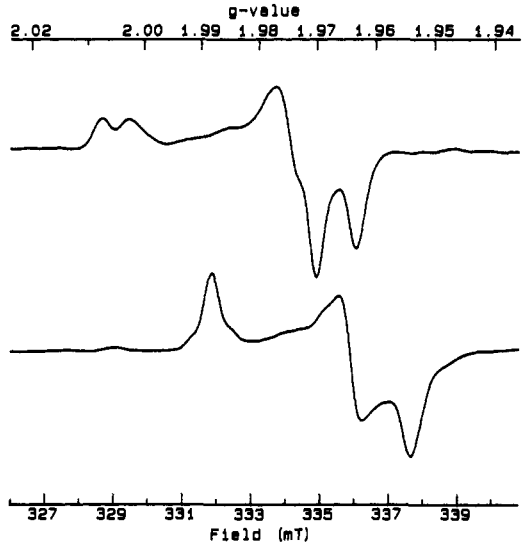

FIGURE 1: EPR spectra of the high-pH (upper trace) and low-pH/Cl^- (lower trace) samples used for the X-ray spectroscopy measurements. Spectrometer conditions were 9.233 GHz, 5 mW of applied power, and a modulation amplitude of 0.1 mT. The sample temperature was 96 K.

and phenazine as redox mediators, as described by Dutton (1978). Samples in the Mo(IV) oxidation state were prepared by adjusting the potential to approximately −360 mV at pH 6 and −540 mV at pH 9. Samples for X-ray spectroscopy were prepared in 10 mm × 10 mm × 3 mm Lucite cells and kept at liquid nitrogen temperatures until data collection; final molybdenum concentrations were approximately 1 mM.

EPR spectroscopy used a Varian E-109 instrument interfaced to an ACT Apricot Xi computer. EPR integrations were performed with respect to a Cu–ethylenediaminetetraacetate standard, with corrections for g value (Aasa & Vänngård 1978), and gave values of 73% and 76% Mo(V) for the high- and low-pH samples, respectively. Thus, approximately three-fourths of the molybdenum in both samples was in the Mo(V) oxidation state, the remainder presumably being a mixture of Mo(IV) and Mo(VI) in unknown proportions.

The line shapes of the Mo(V) EPR signals of the Mo(V) samples were used as an index of sample homogeneity and are shown in Figure 1. The Mo(V) component of both samples was essentially all in the desired form, the EPR spectra of the samples being free of any noticeable amounts of signals from other species (Figure 1).

Data Collection. X-ray absorption spectroscopy was performed at the Stanford Synchrotron Radiation Laboratory by using beam lines IV-2 and VII-3, with Si(220) double-crystal monochromators and the electron storage ring SPEAR operating in dedicated mode (3.0 GeV, 30–70 mA). The spectrometer was calibrated by using the first inflection point of a molybdenum foil standard (defined as 20003.9 eV) that was simultaneously recorded with the data by using a three ion chamber geometry. X-ray absorption was monitored by measuring the X-ray fluorescence excitation spectrum using an array of NaI scintillation detectors (Cramer & Scott, 1979) or a solid-state germanium detector array (Cramer et al., 1988), together with appropriate thickness Zr filters and a slit assembly. For the Ge detector, individual array elements were operated at maximum count rates of approximately 75 kHz, and corrections for instrumental dead-time effects were applied as previously described (Cramer et al., 1988). Samples were maintained at a temperature close to 4 K in an Oxford Instruments CF1204 liquid helium flow cryostat during data collection.

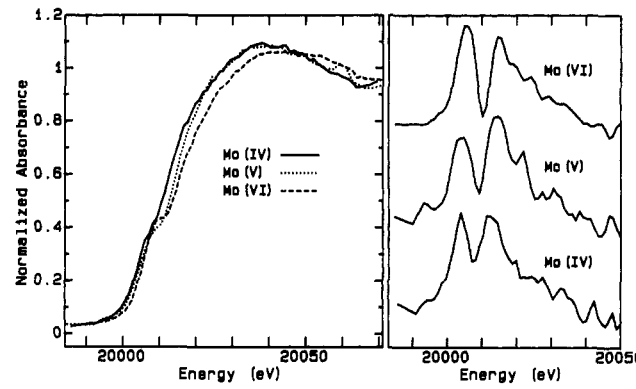

FIGURE 2: (Left) Molybdenum K-edge spectra of the low-pH/Cl^- sample predominantly in the Mo(VI) (---), Mo(V) (···) and Mo(IV) (—) oxidation states. (Right) First derivative Mo K-edge spectra of, from top to bottom, Mo(VI), Mo(V), and Mo(VI) samples.

Data Analysis. The EXAFS oscillations $\chi(k)$ were extracted from the raw data by using standard techniques [e.g., Cramer et al. (1981)] and were quantitatively analyzed by curve fitting to the approximate expression

$$\chi(k) \simeq \sum_b [N_b A_{ab}(k)/kR_{ab}^2] e^{-2\sigma_{ab}^2 k^2} \sin(2kR_{ab} + \alpha_{ab}(k)) \quad (1)$$

in which k is the photoelectron wave vector, N_b is the number of b-type atoms at a distance R_{ab} from the absorber atom a with a root mean square deviation σ_{ab} in R_{ab}. $A_{ab}(k)$ and $\alpha_{ab}(k)$ are the amplitude and total phase shift functions, respectively. The threshold energy (E_0) was assumed in all cases to be 20025 eV, and no shifts in E_0 were required in the curve fitting. Values for the functions $A_{ab}(k)$ and $\alpha_{ab}(k)$ were derived from model compounds [$(NH_4)_2MoS_4$ for Mo–S interactions and Na_2MoO_4 for Mo–O interactions] by using σ values calculated from vibrational spectra, as described by Cramer (1981). Comparisons of these experimentally derived phase shift functions with both plane-wave (Teo & Lee, 1979) and curved-wave (McKale et al., 1988) theoretical functions (the latter being appropriately corrected for R) indicated systematic differences, which would yield an overestimate in R of +0.02 Å if theoretical phase shifts were used.

Results and Discussion

Edge Spectra. The molybdenum K-edge spectra of the three different oxidation states of the low-pH/Cl sample are illustrated in Figure 2. There is a shift of approximately −2 eV in the apparent edge position per unit decrease in formal oxidation state, which is most apparent in the derivative plot (Figure 2). This is expected for molybdenum species that are ligated to similar ligand types [e.g., Cramer (1978)], although the magnitude of the shift is expected to be quite dependent upon the molybdenum coordination environment. It is thus difficult to derive chemical information from the extent of the shift, but the spectra are consistent with the samples being essentially in the required oxidation states.

All the spectra possess a shoulder at about 20009 eV, which is emphasized in the derivative plots as a peak at about 20005 eV (Figure 2). This is the so-called oxo-edge absorption, which is characteristic of species possessing Mo=O groups (or, to a lesser extent, Mo=S groups); it arises from formally dipole forbidden 1s → 4d bound-state transitions to antibonding orbitals directed principally along Mo=O bonds (Kutzler et al., 1980). The strong presence of this feature here implies Mo=O ligation for all three oxidation states of the molybdenum.

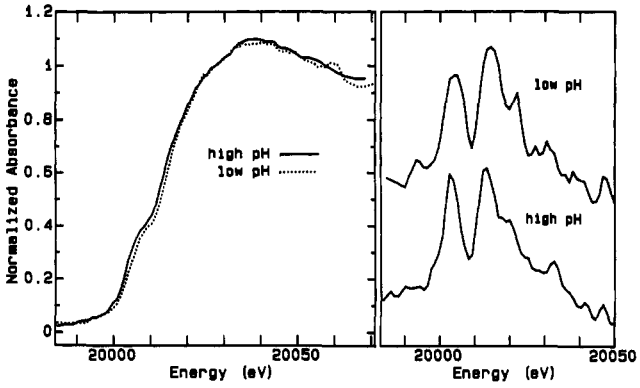

FIGURE 3: Molybdenum K-edge spectra (left) and first derivatives (right) of sulfite oxidase predominantly in the Mo(V) oxidation state in the high- and low-pH forms.

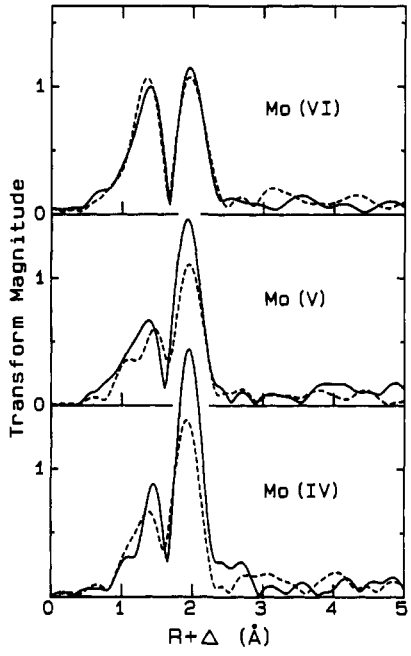

FIGURE 4: Comparison of the EXAFS Fourier transforms for the high-pH (---) and the low-pH/Cl^- (—) samples for Mo(VI), Mo(V), and Mo(IV) oxidation states. A k range of 4–14 $Å^{-1}$ with k^3 weighting was used in all transforms.

No significant differences were observed between the edge spectra of Mo(VI) high- and low-pH samples (not illustrated), and at most only very subtle differences are present for the Mo(V) samples, which are compared in Figure 3 (unfortunately, no edge spectrum for the Mo(IV) high-pH sample was obtained). The similarity of the Mo(V) and Mo(VI) high- and low-pH edge spectra indicates that there are no major changes in the molybdenum environments between high- and low-pH forms.

EXAFS Fourier Transforms and Curve Fitting. The EXAFS Fourier transforms of high- and low-pH samples of the three different oxidation states are compared in Figure 4. Two major features are present in all of the transforms, at $R + \Delta = 1.3$ Å and at $R + \Delta = 2.0$ Å; these are attributable to Mo=O and chiefly to Mo—(S/Cl)[1] interactions, respectively. The Mo(VI) oxidation state of the enzyme shows essentially no change between high- low-pH samples, the data being indistinguishable within the limits of the noise. EXAFS curve-fitting results (Figure 5, Table I) confirm the similarity

[1] Note that EXAFS cannot distinguish between scatterers of similar atomic number, such as sulfur and chlorine or oxygen and nitrogen.

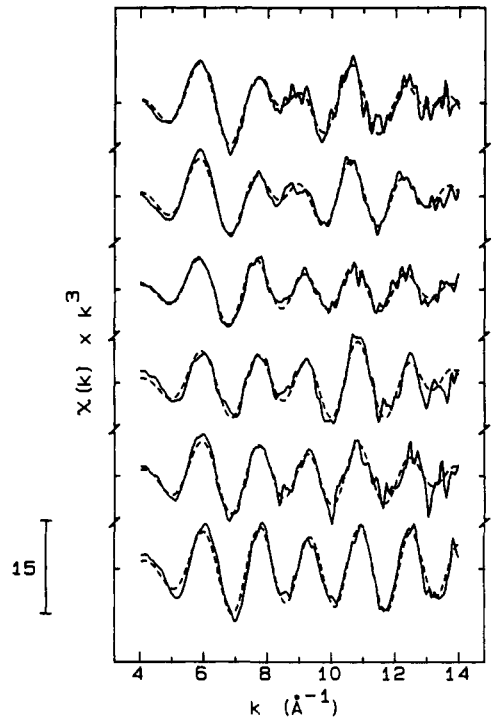

FIGURE 5: EXAFS spectra (—) plus fits (---) for, from top to bottom, Mo(VI) high-pH, Mo(VI) low-pH/Cl^-, Mo(V) high-pH, Mo(V) low-pH/Cl^-, Mo(IV) high-pH, and Mo(IV) low-pH/Cl^- forms. All experimental curves have been slightly smoothed by convolution with a Gaussian of width 0.07 $Å^{-1}$.

of the data. In contrast, both the Mo(V) and Mo(IV) samples show significant differences in the EXAFS spectra of high- and low-pH samples; both possess a stronger Mo—(S/Cl) peak in the EXAFS Fourier transform of the low-pH sample.

The Mo(VI) data could be fitted adequately with two shells [Mo=O and Mo—(S/Cl)], although some improvement was achieved by including an additional oxygen (or nitrogen) interaction (Table I). The Mo(V) and Mo(IV) data required three shells for an adequate fit. The most chemically reasonable assignment for the long Mo–(O/N) interaction in the Mo(V) and Mo(IV) data is an Mo—OH group arising from protonation of one of the Mo=O groups of the Mo(VI) form. The presence of such a ligand for the Mo(V) forms has previously been suggested from EPR spectroscopy [cf. Bray (1980, 1988) and George (1985)].

The Mo=O bond lengths found here deserve some comment in the light of the recent paper of Mayer (1988). For the Mo(VI) oxidation state, our estimate of the Mo=O bond lengths of 1.70 Å (Table I) compares well with his weighted mean of 1.70 Å from 162 Mo(VI) dioxo species. Similarly, the Mo(IV) species (both 1.69 Å, Table I) and the Mo(V) low-pH species (1.68 Å, Table I) compare with Mayer's weighted mean for 19 monooxo Mo(IV) compounds of 1.68 Å and 73 monooxo Mo(V) compounds of 1.68 Å. The Mo(V) high-pH species, however, has an unusually long Mo=O bond length of 1.72 Å (Table I); while this is within the range found for Mo(V) monooxo compounds (Mayer, 1988), the fact that the bond has lengthened on reduction (with concomitant loss of an Mo=O bond, Table I) is unexpected. While the change is within the systematic EXAFS uncertainty of ±0.02 Å [arising primarily from nontransferability of $\alpha_{ab}(k)$ in eq 1], the relative accuracy among chemically similar species is on the order of 0.01 Å, and we therefore believe that the lengthening is significant: it is difficult to explain this in simple chemical terms, but it probably indicates that more than simple redox chemistry is occurring in the reduction process.

Table I: EXAFS Curve-Fitting Results[a]

sample	Mo=O			Mo—(S/Cl)			Mo—(O/N)			
	N	R (Å)	σ (Å)	N	R (Å)	σ (Å)	N	R (Å)	σ (Å)	F^b
Mo(VI), high pH	2	1.704	0.044	2	2.417	0.037				1.78
	2	1.704	0.045	3	2.416	0.058				1.67
	2	1.705	0.047	4	2.416	0.072				1.80
	2	1.703	0.044	3	2.415	0.057	1	2.059	0.041	1.22
conclusion	2	1.70		~3	2.42					
Mo(VI), low pH	2	1.703	0.049	2	2.418	0.035				1.53
	2	1.703	0.050	3	2.417	0.056				1.43
	2	1.704	0.052	4	2.417	0.070				1.58
	2	1.702	0.054	3	2.416	0.057	1	2.050	0.039	0.81
conclusion	2	1.70		~3	2.42					
Mo(V), high pH	1	1.719	0.054	2	2.410	0.038	1	2.160	0.062	0.60
	1	1.714	0.048	3	2.405	0.065	1	2.053	0.082	0.60
	1	1.722	0.058	4	2.405	0.074	1	2.059	0.076	0.63
	0.9	1.722	0.018	2.5	2.409	0.052	1	2.151	0.080	0.60[c]
conclusion	1	1.72		2–3	2.41		~1	~2.1		
Mo(V), low pH	1	1.677	0.000	2	2.385	0.019	1	1.975	0.066	1.03
	1	1.675	0.023	3	2.385	0.047	1	1.980	0.044	0.90
	1	1.672	0.032	4	2.385	0.063	1	1.984	0.025	1.03
	1.2	1.676	0.042	3.3	2.385	0.052	1	1.975	0.040	0.87[c]
conclusion	1	1.68		3–4	2.39		~1	1.98		
Mo(IV), high pH	1	1.688	0.043	2	2.388	0.024	1	2.163	0.035	1.60
	1	1.687	0.046	3	2.383	0.051	1	2.138	0.093	1.47
	1	1.689	0.048	4	2.383	0.063	1	2.050	0.090	1.55
	0.9	1.687	0.042	3.2	2.383	0.052	1	2.124	0.096	1.46[c]
conclusion	1	1.69		~3	2.38		~1	~2.1		
Mo(IV), low pH	1	1.693	0.042	2	2.370	0.000	1	2.101	0.085	2.01
	1	1.694	0.042	3	2.368	0.032	1	2.044	0.041	0.71
	1	1.694	0.042	4	2.366	0.044	1	2.025	0.039	0.71
	1.0	1.693	0.042	4.4	2.365	0.052	1	2.019	0.010	0.67[c]
conclusion	1	1.69		~4	2.37		~1	2.0		

[a] In general, N was held an integer, while R and σ were allowed to vary (but see footnote *c*). For the Mo=O and Mo—(S/Cl) shells, the estimates of coordination numbers (N) and σ are considered accurate to about 30%, while values for R have a systematic error of about ±0.02 Å. These uncertainties are higher for the Mo—(O/N) shell (which gives the weakest EXAFS) because of correlation with the intense Mo—(S/Cl) EXAFS in the curve-fitting process. It is possible that additional long Mo—(O/N) interactions may be undetected. [b] The fit-error function F is defined as $[\sum(\chi_o - \chi_c)^2 k^6]/n$, where χ_o and χ_c are the observed and calculated EXAFS, respectively, n is the number of data points included in the fit, and the summation is over all n points. [c] σ for the Mo=O and Mo—(S/Cl) shells was fixed at chemically reasonable values, while N for these interactions was allowed to vary in the fit.

The results of the present EXAFS analysis contrast in some respects with those reported earlier (Cramer et al., 1979a, 1981), and this deserves some comment. The largest discrepancy is for the EXAFS of the Mo(V) oxidation state. Lamy et al. (1980) have previously noted that the earlier Mo(V) samples (Cramer et al., 1979a) probably contained less than 50% of this oxidation state, as they were generated by simple addition of sulfite. Our conclusion that the Mo(V) oxidation state possesses a single oxo ligand (Table I) contrasts with the earlier estimate of two such ligands (Cramer et al., 1979a). This discrepancy suggests heterogeneity in the earlier samples, with a large fraction of the dioxo Mo(VI) form. While a substantial initial excess of reductant was used in the earlier experiments (Cramer et al., 1979a), it is quite likely that reoxidation occurred during the experiment.

Differences between the current EXAFS results on the Mo(VI) and Mo(IV) states and those previously reported are much less marked. Our estimates for the number of sulfur ligands are in agreement with the earlier work, and all bond lengths agree within 0.01 Å (Table I; Cramer et al., 1981). Some discrepancies might be expected because previous experiments were carried out in phosphate buffer and at ambient temperatures (Cramer et al., 1981). The effect of the latter is that our values for σ are consistently smaller than those of Cramer et al. (1981), which is expected from freezing out vibrational components of σ. The effects of phosphate buffer, however, are potentially rather more serious. Phosphate has long been known to be a potent inhibitor of sulfite oxidase which, at least for the Mo(V) state, binds to molybdenum (Gutteridge et al., 1980; George et al., 1988). Nevertheless, the overall similarity of the present EXAFS results and those of Cramer et al. (1981) means that the effects of phosphate upon the Mo(VI) and Mo(IV) oxidation states are, if present, quite subtle.

Structural Basis of the High-pH–Low-pH Transition. Previous information on the structure of the high-pH and low-pH species has been inferred entirely from EPR spectroscopy of the Mo(V) forms. Our data provide the first quantitative structural information on the Mo(V) oxidation states, together with equivalent information on the EPR-silent Mo(IV) and Mo(VI) states. Unfortunately, EXAFS is incapable of distinguishing sulfur and chlorine,[1] so binding of chloride to molybdenum will manifest itself as an apparent increase in the Mo–(S/Cl) coordination number if the Mo–Cl and Mo–S bond lengths are different by less than the EXAFS resolution.[2] Furthermore, the systematic uncertainty in determining the coordination number is about 30%, in part due to correlation of the coordination number and σ in the

[2] The EXAFS resolution ΔR is the smallest discernible difference in R for similar scatterers and is approximately related to the length of the data set by $\Delta R \simeq \pi/2k$; in our case it is about 0.11 Å. Distances differing by less than this would not be individually resolved by the curve-fitting process, but instead would be reflected by an average distance and an apparent increase in σ.

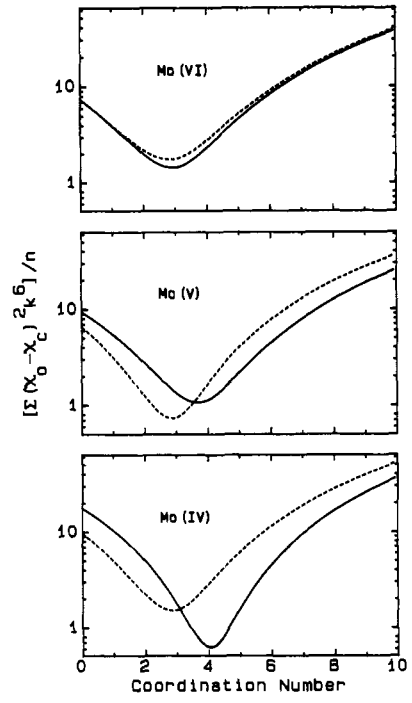

FIGURE 6: EXAFS curve-fitting search profiles of high-pH (---) vs low-pH/Cl^- (—) samples for, from top to bottom, Mo(VI), Mo(V), and Mo(IV) oxidation states. The vertical scale is the fit-error function in which χ_o and χ_c are the observed and calculated EXAFS, respectively, n is the total number of data points, and the summation is over all n points. σ for the Mo–(S/Cl) interaction was held constant at the chemically reasonable value of 0.05 Å. The most appropriate fits are indicated by the minima.

curve-fitting process. We have therefore used search profiles to quantitatively analyze changes in Mo–(S/Cl) coordination number (Figure 6). These convincingly show that under low-pH conditions the apparent Mo–(S/Cl) coordination number increases by approximately one for both Mo(IV) and Mo(V) forms, but not for the Mo(VI) form. We take this as evidence that chloride binds to the molybdenum in the Mo(IV) and Mo(V) forms, but not in the Mo(VI) form, under our conditions. Although unlikely, a very weak chloride coordination to Mo(VI) is difficult to completely exclude on the basis of EXAFS data alone. For all of the data the Mo–(O/N) interaction gives the smallest contribution to the EXAFS and is the least well quantified in terms of both coordination number and bond length. It is important to note that because of this there may not in fact be the overall increase in coordination number upon chloride binding that is implied by our analysis. Thus, the loss of an oxygen or nitrogen ligand upon chloride binding would cause only very small changes to the EXAFS, which might easily be too subtle to be resolved by the curve-fitting analysis. This would be especially true if the original Mo–(O/N) interaction were a relatively distant one (e.g. >2.2 Å). Minimal structures for high- and low-pH forms of all three oxidation states, based on the EXAFS analysis, are shown in Figure 7.

The low-pH Mo(V) EPR signal differs from the high-pH signal in possessing well-resolved hyperfine splitting from a single exchangeable proton (Lamy et al., 1980). Bray et al. (1983) have postulated that the relationship between the high- and low-pH species is

$$\underset{\text{high pH}}{\text{Mo=O}} + \text{H}^+ + \text{Cl}^- \leftrightarrow \underset{\text{low pH}}{\text{Mo(—OH)—Cl}} \qquad (2)$$

where the Mo–OH proton of the low-pH form gives the hyperfine splitting and exhibits the pK_a that influences the

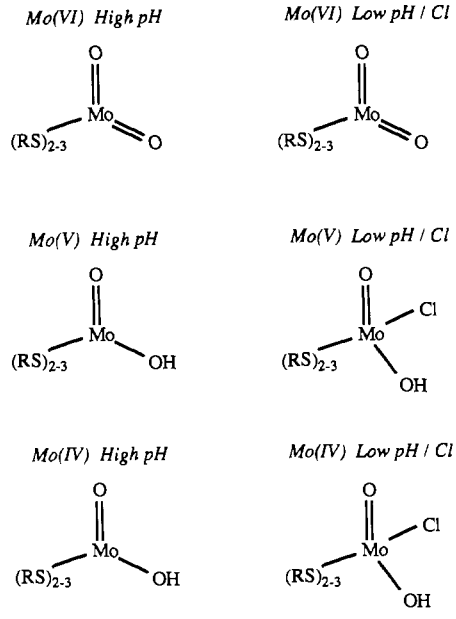

FIGURE 7: Minimal structures for high- and low-pH species in the Mo(VI), Mo(V), and Mo(IV) oxidation states, based on a combination of our EXAFS and earlier EPR results [e.g., Bray (1980, 1988)]. As trigonometric information is usually not directly obtainable from EXAFS, the figure does not indicate geometries. Nevertheless, we expect the two terminal oxo ligands of the Mo(VI) species to be cis to one another, with an O–Mo–O angle near 106° [e.g., see Stiefel (1987)].

equilibrium. Bray et al. (1983) have also observed ^{19}F hyperfine coupling in the EPR spectrum of a Mo(V) low-pH fluoride species, presumed to be analogous to the usual low-pH chloride complex, indicating the presence of Mo–F ligation in the fluoride complex and supporting their hypothesis of Mo–Cl ligation in the normal low-pH species. Later work (George, 1985), however, indicated that the high-pH Mo(V) species also possesses a coupled exchangeable proton. Although this proton does not give resolved splittings of the 9-GHz EPR signal, its presence is revealed by formally forbidden $\Delta M_I = \pm 1$ proton spin–flip transitions in the Mo(V) EPR signal. These results cast doubt on whether the proton whose pK_a influences the equilibrium between high-pH and low-pH forms is in fact that which is observed from its hyperfine coupling in the low-pH EPR signal.

Our data conclusively show that the number of oxo groups remains the same upon transition from high-pH to low-pH form, and thus the process does not involve protonation of an Mo=O group. This aspect of the hypothesis of Bray et al. (1983) (eq 2) is thus disproved. Two alternative schemes that are consistent with all available data are shown in Chart I. Chart Ia is that of George (1985), in which a ligand X (part of the protein or molybdenum cofactor) is protonated on going from high- to low-pH forms, vacating a coordination site that is then occupied by chloride. In the alternative, Chart Ib, chloride and hydroxide simply compete for the same coordination site. Such a competition has been suggested in the iron–chlorin-containing myeloperoxidase (Ikeda-Saito & Prince, 1985). In principal, parts a and b of Chart I could be distinguished by magnetic resonance spectroscopy, since the high-pH form of Chart Ib possesses two exchangeable protons while that of Chart Ia possesses only one. Note that in either case the high- and low-pH forms are misnamed, since the transition between the two forms is primarily a function of chloride concentration: perhaps more appropriate names for the two species would be chloride-free and chloride-bound forms.

Chart I: Possible Relationship between High- and Low-pH Species in the Mo(V) and Mo(IV) Oxidation States[a]

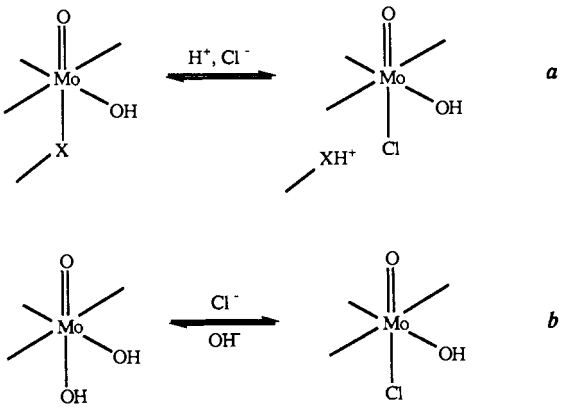

[a] The chloride is indicated as binding axially, because trans effects from the terminal oxo would make ligands in this position labile. For this to be correct, the elongation of the Mo–Cl bond due to the trans effect must be less than the EXAFS resolution.[2] Binding in an equatorial position is, of course, also possible. As discussed in the text, the Mo(VI) oxidation state shows no change between high- and low-pH conditions.

ACKNOWLEDGMENTS

We thank Dr. E. I. Stiefel for helpful comments and the staff of SSRL for their assistance in making this work possible. SSRL is funded by the DOE under Contract DE-AC03-82ER-13000, Office of Basic Energy Sciences, Division of Chemical Sciences, and NIH, Biotechnology Resource Program, Division of Research Resources.

Registry No. Mo, 7439-98-7; sulfite oxidase, 9029-38-3.

REFERENCES

Aasa, R., & Vänngård, T. (1975) *J. Magn. Reson. 19*, 308–315.

Bray, R. C. (1980) *Adv. Enzymol. Relat. Areas Mol. Biol. 51*, 107–165.

Bray, R. C. (1986) *Polyhedron 5*, 591–595.

Bray, R. C. (1988) *Q. Rev. Biophys. 21*, 299–329.

Bray, R. C., Lamy, M. T., Gutteridge, S., & Wilkinson, T. (1982) *Biochem. J. 201*, 241–243.

Bray, R. C., Gutteridge, S., Lamy, M. T., & Wilkinson, T. (1983) *Biochem. J. 211*, 227–236.

Cohen, H. J., & Fridovich, I. (1971) *J. Biol. Chem. 246*, 359–366.

Cramer, S. P. (1978) Ph.D. Thesis, Stanford University.

Cramer, S. P. (1981) in *EXAFS for Inorganic Systems* (Garner, C. D., & Hasnain, S. S., Eds.) Daresbury Laboratory, Daresbury, England.

Cramer, S. P., & Scott, R. A. (1979) *Rev. Sci. Instrum. 52*, 395–399.

Cramer, S. P., Gray, H. B., & Rajagopalan, K. V. (1979a) *J. Am. Chem. Soc. 101*, 2772–2774.

Cramer, S. P., Johnson, J. L., Rajagopalan, K. V., & Sorrell, T. N. (1979b) *Biochem. Biophys. Res. Commun. 91*, 434–439.

Cramer, S. P., Gray, H. B., Scott, N. S., Barber, M., & Rajagopalan, K. V. (1980) in *Molybdenum Chemistry of Biological Significance* (Newton, W. E., & Otsuka, S., Eds.) pp 157–168, Plenum Press, London.

Cramer, S. P., Whal, R., & Rajagopalan, K. V. (1981) *J. Am. Chem. Soc. 103*, 7721–7727.

Cramer, S. P., Tench, O., Yocum, M., & George, G. N. (1988) *Nucl. Instrum. Methods A266B*, 586–591.

Dutton, P. L. (1978) *Methods Enzymol. 54*, 411–435.

George, G. N. (1985) *J. Magn. Reson. 64*, 384–394.

George, G. N., Prince, R. C., Kipke, C. A., Sunde, R. A., & Enemark, J. E. (1988) *Biochem. J. 256*, 307–309.

Gutteridge, S., Lamy, M. T., & Bray, R. C. (1980) *Biochem. J. 191*, 285–288.

Ikeda-Saito, M., & Prince, R. C. (1985) *J. Biol. Chem. 260*, 8301–8305.

Kessler, D. L., & Rajagopalan, K. V. (1972) *J. Biol. Chem. 247*, 6566–6573.

Kipke, C. A., Cusanovich, M. A., Tollin, G., Sunde, R. A., & Enemark, J. H. (1988) *Biochemistry 27*, 2918–2926.

Kipke, C. A., Enemark, J. H., & Sunde, R. A. (1989) *Arch. Biochem. Biophys.* (in press).

Kutzler, F. W., Natoli, C. R., Misemer, D. K., Doniach, S., & Hodgson, K. O. (1980) *J. Chem. Phys. 73*, 3274–3288.

Lamy, M. T., Gutteridge, S., & Bray, R. C. (1980) *Biochem. J. 185*, 397–403.

Mayer, J. M. (1988) *Inorg. Chem. 27*, 3899–3903.

McKale, A. G., Veal, B. W., Paulikas, A. P., Chan, S.-K., & Knapp, G. S. (1988) *J. Am. Chem. Soc. 110*, 3763–3768.

Stiefel, E. I. (1987) in *Comprehensive Coordination Chemistry* (Wilkinson, G., Gillard, R. D., & McCleverty, J. A., Eds.) pp 1375–1421, Pergamon Press, New York.

Teo, B.-K., & Lee, P. A. (1979) *J. Am. Chem. Soc. 101*, 2815–2832.